Evaluation of Two Multi-Fidelity Optimization Frameworks in MDO Results Including Aeroelasticity and Aeroacoustics

José Lobo do Vale
University of Victoria
3800 Finnerty Rd, Victoria, BC
CANADA

joselobodovale@uvic.ca

Martin Sohst
University of Victoria
3800 Finnerty Rd, Victoria, BC
CANADA

Frederico Afonso
Universidade de Lisboa
Av. Rovisco Pais, 1, 1049-001 Lisbon
PORTUGAL

Fernando Lau
Universidade de Lisboa
Av. Rovisco Pais, 1, 1049-001 Lisbon
PORTUGAL

Keywords: Multi-fidelity models; Gaussian processes; compositional kernels; uncertainty quantification; early-stage design.

ABSTRACT

The use of different levels of fidelity in the design and optimization process can support an accelerated development of aircraft. Despite high-fidelity models providing higher accuracy, they represent expensive calculations while low-fidelity assessments can be executed with less costs and precision. Combining fidelities can be beneficial since information from the low-fidelity evaluations can be used to reduce the number of high-fidelity evaluations. Both Multi-fidelity Kriging and Deep Neural Network-Multi-fidelity Bayesian Optimization have been used in surrogate based multi-fidelity MDO. It is therefore of interest to understand which approach is more likely to produce optimal results with the least computational effort. In this work the two approaches are introduced and compared using test functions to estimate a trend for their performances in MDO. Then the approaches are applied to aeroacoustic and aerostructural optimizations in order to verify if they hold in more realistic problems. The multi-fidelity Kriging outperforms the single fidelity in every case for the test functions, underlining the usefulness of a multi-fidelity framework in comparison to a single fidelity one.

1.0 INTRODUCTION

Multi-fidelity (MF) methods for optimization have known intense developments in recent years. MF Gaussian Process-Upper Confidence Bound (MF-GP-UCB) (Kandasamy, 2016, Kandasamy, 2017), MF Kriging optimization (Rumpfkeil, 2020) and MF-Mutual Information-Greedy (MF-MI-Greedy) (Song, 2019) are examples of developed frameworks using Gaussian Process (GP) as surrogate models and different fidelity tools to limit the computational costs incurred during optimizations.

In Kandasamy (2016) the authors present a formalism for multi-fidelity bandit optimization using GP assumptions and developed the MF-GP-UCB algorithm for that purpose, proving that it explores the space with low fidelity and successfully zooms in smaller regions near the optimum for higher fidelity evaluations, reducing the regret compared to single fidelity strategies. Further developments in this framework (Kandasami, 2017) eliminate some of its shortcomings, like the limitation to a uniform bound between lower and higher fidelities, the separation between information stemming from each fidelity level and it handles continuous approximations. However, it still requires the low and high-fidelity models to be strongly correlated, as otherwise no beneficial behaviour is obtained.

Recently the MF-MI-Greedy (Song, 2019) proposal prioritizes maximizing the amount of mutual information gathered between fidelities and introduces a simple notion of regret that includes the different fidelity costs. It is proved that the framework achieves low regret and that improved performance relative to the MF-GP-UCB can be obtained.

MF Kriging approaches are employed for engineering problems as a part of Gaussian Processes. An in-depth exploration of multi-fidelity methods and the use of multi-level data is found in Fernández-Godino (2019). Low-fidelity results are utilized to improve the prediction quality of the high-fidelity model. A correlated low-fidelity model can support an accelerated identification of regions containing global or local optima, reducing computational cost due to reduced expensive evaluations. Scaling functions are a robust way to fuse the information of low-fidelity models and are employed in the comparison with other approaches for multi-fidelity assessments (Fernández-Godino, 2019). Another possibility are low-fidelity regression models utilized as mean approximations for high-fidelity Gaussian processes. However, they are less robust for higher number of dimensions and sample points and their initial advantage of utilizing the low-fidelity information diminishes more rapidly. Thus, in this work a bridge function approach is used for comparative studies.

An alternative to GP in multi-fidelity methods for optimization is the usage of Deep Neural Networks. The Deep Neural Network-Multi-Fidelity Bayesian Optimization (DNN MFBO) (Li, 2020) is one of such methods. In the proposed approach, complex and non-linear relationships between the fidelities are captured to improve objective function estimation, mitigating possible oversimplifications of said relationships.

Neural Networks (NN) have been used in aircraft design for about then 3 decades or earlier. In 1993, Berke et al. (1993) have used NN to perform structural optimization on different wing shape configurations.

More recently, NN have been associated to the algorithms identified as Artificial Intelligence and Machine Learning, where massive amounts of data are used in order to enable computers to predict human behaviour, associated to social networks, and perform speech and visual recognition tasks. These developments in turn generated open-source codes accessible to the general public, sparking an interest from the aircraft design research and engineering community in its use for design processes and other areas (aircraft maintenance, for example).

In 2016, an extensive database of 100,000 was used to train a NN surrogate model for the prediction of lift and drag coefficients in a wing and tube configuration (Secco, 2015). An optimization using these trained NN as a surrogate model proved to cost orders of magnitude less than a traditional physics model-based optimization with similar optimal design outcomes. A study comparing the adjoint-based optimization with NN gradient based optimization and with NN Bayesian optimization for aerodynamic optimization of airfoils (Renganathan, 2021) showed a significant reduction in the computational costs for both the NN gradient based and NN Bayesian optimization relative to the adjoint based optimization. Nevertheless, the NN based optimizations efficiency decreases with the dimensionality of the problem, which does not affect the adjoint-based optimization. A review of the deep learning methods including deep neural network, deep autoencoder, deep belief network, convolutional neural network, and recurrent neural network and their applications to aircraft design, dynamics and control can be found in (Dong 2018).

In the preliminary aircraft design process, one aims at obtaining physics-based insight in a multidisciplinary environment early in the process. Therefore, the employment of high-fidelity methods becomes more important, even though computationally expensive. Alleviating computational costs and joining information of low- and high-fidelity assessments can provide an accelerated and improved design. Examples of the multi-fidelity approach utilization for MDO in aircraft design can be found for BO approaches (Meliani, 2019) and NN approaches (Zhang, 2020). However, often single fidelity models are employed, as their implementation is simpler and the relation between low- and high-fidelity models requires more insight to properly set up (Fernández-Godino, 2019).

In this paper, we propose to evaluate and compare a MF Kriging and DNN-MFBO performances in a physics based multi-fidelity MDO context. Figure 1 shows the standard process for a surrogate based optimization approach. With an initial database of evaluated samples, surrogate models are built. In the specific case of a multi-fidelity approach those can include low-, high- and mixed-fidelity models, where information of all involved fidelities is utilized to obtain a surrogate model with the best predictive capabilities possible. One or multiple surrogates are then employed to obtain a new candidate design at which the real expensive functions are evaluated, and the result is fed back into the data base. If the assessed design shows a convergence behaviour and is satisfactory with respect to objective and feasible with respect to the constraints, the optimization is terminated. Otherwise, the surrogate models are rebuilt with the new information and the process repeats.

Starting with a short explanation of the multi-fidelity approaches and providing details about the different methods, the paper continues with an example of multi-fidelity optimizations on a test function and continues with MF MDO applications to aeroacoustic and aerostructural optimization problems. The paper is finalized with the concluding remarks about the performances of the MF Kriging and the DNN-MFB.

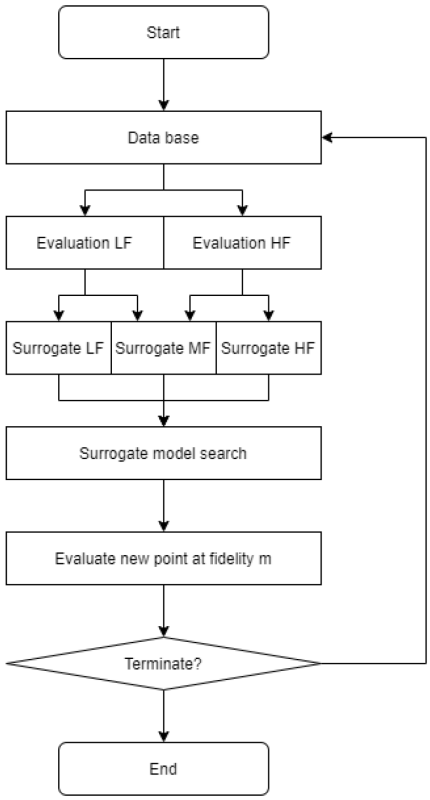

Figure 1: The typical surrogate process.

2.0 BAYESIAN OPTIMIZATION IN MULTI-FIDELITY MDO

The Gaussian process assumes the mean value μ with the deviation σ.With a spatial correlation function a model can be built based on a limited number of observations. In Kriging approaches, the Gaussian correlation function is a popular choice, as it is in this work, and expressed as:

$$\psi\left(x^{(i)}, x^{(l)}\right) = \exp\left(-\sum_{j=1}^{k} \theta_j \left(x_j^{(i)} - x_j^{(l)}\right)^2\right) \tag{1}$$

The parameter θ, determined by maximizing the likelihood to fit the present data, shapes the surrogate model. A new prediction can then be obtained by:

$$\hat{y}(x) = \hat{\mu}(x) + \psi^T \Psi^{-1}\left(y - \hat{\mu}(x)\right) \tag{2}$$

For a multi-fidelity approach employing bridge functions, one assumes a correlation between the low- and high-fidelity evaluations, where the difference can be modelled by an independent additional surrogate.

The high-fidelity results are therefore estimated as:

$$\hat{y}_{HF} = \hat{y}_{LF}(x) + \hat{\delta}(x) \tag{3}$$

where $\hat{\delta}(x)$ is the bridge function surrogate, correcting the difference between the low- and high-fidelity evaluations, and the low-fidelity model provides the low-fidelity estimations. It is assumed here that the low-fidelity evaluations, while less expensive than the high-fidelity evaluations, are utilized to generate a surrogate model nevertheless.

If a Gaussian model is employed for the correction, the assumptions applying to the bridge model are similar to the general idea of Gaussian processes. Thus, the expected difference, often based on differences of the evaluated physics on the fidelities, is modelled as a mean value with stochastic deviations. Therefore, this additive response provides a robust correction to consider the low-fidelity information on a global scale with the discrepancies between the high- and low-fidelity being corrected locally.

An important aspect of the employment of surrogate models in MDO is the intended cost reduction of expensive evaluations. However, depending on the nature of the real function, a high number of costly assessments might be necessary to obtain a globally accurate model of the real function. Thus, in MDO the goal is more likely to quickly identify regions of local and global minima rather than obtaining a global accurate representation. Further, with increasing number of evaluated designs the computational costs of building a model increases due to the increased size of the correlation matrix and the necessary inversion. Also, an increase in costs is also present with increased dimensions of the problem, a reason why the application is often limited to lower dimensionality problems. However, approaches like partial least square (PLS) Kriging (Bouhlel, 2016) allow for a cost improvement due to internal dimensionality reduction.

Another essential aspect of surrogate modelling is the achieved accuracy of the model. With the mathematical replacement one aims to obtain a close representation of the replaced function to be used for design space exploration and optimization. The utilization of multiple levels of fidelity can in general improve the accuracy. However, an error is still present throughout the design space that will only decrease with more information (evaluations of the real function) being incorporated. Still, it is a question of the goal for the surrogate, if the model should be accurate over the whole design space or if it is sufficient to be accurate only in regions of interest, for instance areas of minima. This again will influence the overall computational costs.

3.0 DEEP NEUTRAL NETWORK MUTI-FIDELITY MDO METHODOLOGY

In this work, we tried to reproduce the methodology for the DNN-MFBO described in (Li, 2020). In their work, the multi-fidelity model is intended to capture complex relationships between fidelities based on NN built for each fidelity that use as input the output of the previous fidelity NN. Figure 2 depicts the sequence of NN models as the fidelity is increased.

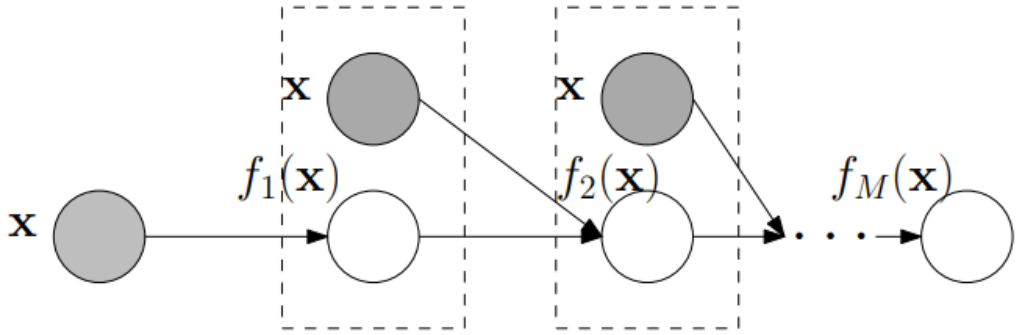

Figure 2: Multi-fidelity NN models. The output of each fidelity NN model is used together with the model input x as input for the next fidelity NN model (reproduced from (Li, 2020).

For each fidelity the NN is parameterized by the weights of the last layer (w_m) and the remaining training parameters in the NN (θ_m) such that the model for fidelity *m* becomes (Li, 2020):

$$f_m(x) = w_m^T \phi_{\theta_m}(x_m), \qquad y_m(x) = f_m(x) + \epsilon_m \tag{4}$$

where $\phi_{\theta_m}(x_m)$ is the output of the second to last layer and $\epsilon_m \approx N(0, \sigma_m^2)$ is Gaussian noise.

3.1 DNN-MFBO Training

The DNN-MFBO model is trained by defining and maximizing a variational model Evidence Lower Bound (ELBO). Firstly one assigns of a normal prior to each w_m, which given a samples set establishes the joint probability for the model as $p(W, Y|X, \theta, s) = \prod_{m=1}^{M} N(w_m|\mathbf{0}, \boldsymbol{I}) \prod_{n=1}^{N_m} N(y_{nm}|f_m(x_{nm}), \sigma_m^2)$, where Y and X are training set D outputs and inputs respectively, $W = \{w_m\}$, $\theta = \{\theta_m\}$, $s = \{\sigma_m^2\}$, and $\{y_{nm}, x_{nm}\}$ the nth output-input pair for fidelity m. M and N_m are the maximum fidelity and the number of samples for fidelity m, respectively.

Secondly, a multivariate Gaussian posterior $q(w_m) = N(w_m|\mu_m, \Sigma_m)$ is introduced for each w_m and it is assumed that $q(W) = \prod_{m=1}^{M} q(w_m)$. The ELBO is then constructed as:

$L(q(w), \theta, s) = E_q[\log(p(W, Y|X, \theta, s)/q(w)]$.

Further details on the formulation and computation of the ELBO can be found in (Li, 2020).

Figure 3 depicts the initial samples for the different fidelities and the corresponding NN model after training based on those samples. Notice that the different fidelities present complex relationships with the high fidelity (negative) Branin function. It is apparent that training the NN by maximizing the constructed ELBO produces an output that identifies general trends of the high fidelity function with scarce high fidelity information.

Nevertheless, finding a suitable NN model architecture and tuning the training parameters is a non-trivial task of which the model outcomes depend on. Additionally, it is apparent that the sampling has a very significant influence on the outcome, with different samples producing very different model results for the same architecture and training parameters.

3.2 DNN-MFBO Acquisition Function

In order to find the fidelity and input location the acquisition function to be maximized is:

$$a(x,m) = \frac{1}{\lambda_m}\left(H(f_m(x)|D) - E_{p(f^*|D)}[H(f_m(x)|f^*,D)]\right) \tag{5}$$

where λ_m is the fidelity cost, $f^*$is the maximum of the high fidelity model and $H(\cdot\,|\,\cdot)$ is the conditional entropy of the probability density distribution $p(\cdot\,|\,\cdot)$. This is the *max-value entropy search* function which when maximized provides the maximum information gain on f^*. The computational implementation follows (Li, 2020) and (Takeno 2020).

The computation of the acquisition function requires the approximation of the second term in (5) which is intractable using a Monte-Carlo approximation and further substituting $H(f_m(x)|f^*,D)$ by $H(f_m(x)|f_M(x) \leq f^*,D)$.

The computation of the acquisition function requires the generation of an arbitrary number of approximating instances of f^* that requires running a maximization algorithm for each instance and the calculation of integral quantities using Gauss-Hermite quadrature approximations. This makes the maximization of the acquisition function somewhat expensive to evaluate. Furthermore, the quality of the NN model approximation after training has a significant effect in the subsequent calculation of sample instances of f^* and in the posterior approximations for each fidelity that represent additional complexities in the application of this method.

4.0 DESCRIPTION OF THE APPLICATION PROBLEMS

Firstly, an assessment of the advantages of the multi-fidelity approach relative to a single fidelity approach is made resorting to the optimization of analytical test functions. Both MF-Kriging and DNN-MFBO are used, and their performances compared.

Additionally, two Multidisciplinary Design Optimization (MDO) problems are defined to further investigate the MF-Kriging framework in two simplistic engineering problems for MDO application.

One problem consists in minimizing a weighed function of the perceived noise at a given observer position and the rotor mass by optimizing the geometry of a rotor for a Vertical Take-Off and Landing (VTOL) vehicle at hover conditions. As the high-fidelity model, two semi-empirical models are chosen, one for rotational noise and another for the convected wake of the rotor, following Brown (2018). Regarding the low fidelity model just the rotational noise is accounted for.

The other problem is defined for the minimization of the mass of a flexible High Aspect Ratio aircraft wing subject to structural integrity constraints during its response to a gust load. Only structural variables are considered, and two levels of fidelity are used in the optimization. A transient analysis to determine the gust response is used based on a panel method formulation coupled with an Equivalent Beam Model (EBM) for the wing structure using two-way Fluid-Structure Interaction (FSI) with courser structural and aerodynamic meshes is used as the lower fidelity model while finer meshes results are used as the higher fidelity model. For this problem, only an assessment of the global accuracy of the LF-Kriging approximation was performed at this point.

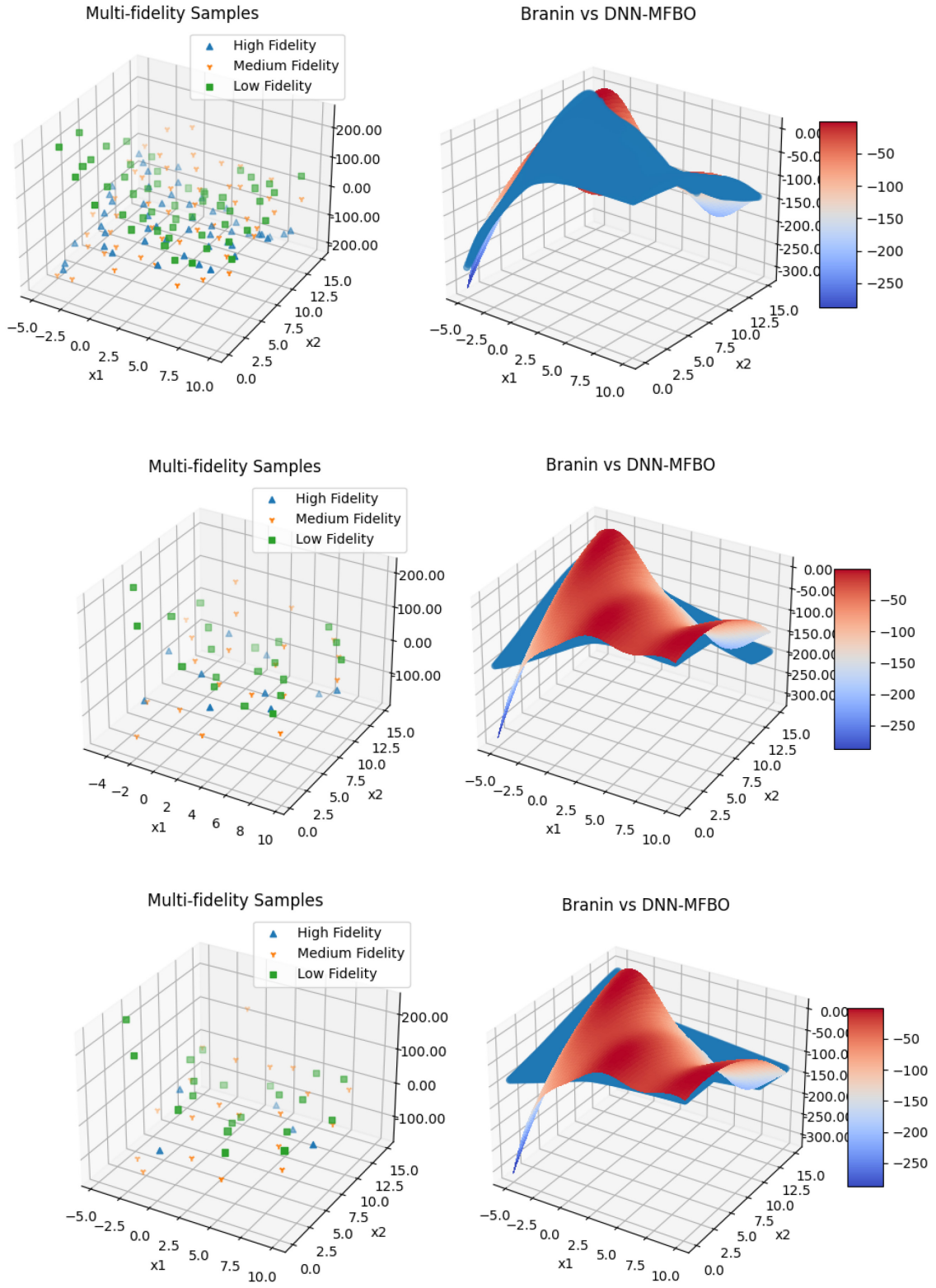

Figure 3: MF samples (left) and comparison between the negative of Branin function and the trained DNN-MFBO model (right). Top – 50 samples for each fidelity; Middle – 20 LF, 20 Medium F, 10 HF samples; Bottom – 20 LF, 20 MF, 5 HF samples. LF, Medium F and HF functions detailed in (Li, 2020).

4.1 Test Function and Resulting Models

The idea of joining low and high-fidelity models is presented on a simple one-dimensional example, taken from Sobester (2008). A high-fidelity function $f(x)$ is given as:

$$f(x) = (6x - 2)^2 * sin(12x - 4) \tag{6}$$

a correlated low-fidelity function that incorporates some of the information but lacks accuracy is given as:

$$f_{LF}(x) = 0.5(6x - 2)^2 * sin(12x - 4) + 10(x - 0.5) - 5 \tag{7}$$

Figure 4 shows the two functions. A distinctive global minimum is present for the high-fidelity function with one local minima. The low-fidelity function presents a global minimum at a different location with the region of a local optimum being similar to the high-fidelity region of the global optimum.

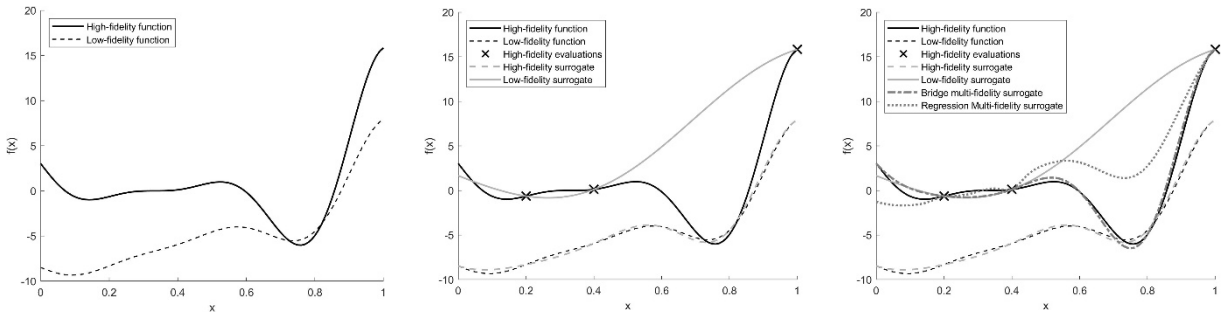

(a) Real functions **(b) Single fidelity surrogates** **(c) Multi-fidelity surrogates**

Figure 4: Example for multi-fidelity responses and generated models for a one-dimensional function.

If the design space is now sampled at specific locations, one can build a surrogate model. As the low-fidelity model is cheaper to evaluate, a denser sampling can be performed, resulting in a closer match of the graphs (see Figure 4b). Thus, the low fidelity surrogate is a good representation of its real equivalent, while the high-fidelity surrogate is far off.

The information can now be utilized to obtain meta-models, with information of both functions. Figure 4c shows two different ways of multi-fidelity surrogates, one is the utilization of a bridge function, where differences of the evaluations are employed. Another possibility is the use of an adapted regression based on the low fidelity model.

A more thorough test case is presented for a 2D function, the adapted Branin function (Sobester, 2008). The high-fidelity function is formulated as:

$$f(x) = \left(15x_2 - \frac{5.1}{4\pi^2}(15x_1 - 5)^2 + \frac{5}{\pi}(15x_1 - 5)^2 - 6\right)^2 + 10\left(1 - \frac{1}{8\pi}\right)cos(15x_1 - 5)^2 + \frac{35}{3} + \frac{1}{3}(15x_1 - 5)^2 \tag{8}$$

and the low-fidelity function as:

$$f(x) = 200 * (x_1 - 0.5)^2 + (x_2 - 0.5)^2 + 1.875(x_1 - 0.5)(x_2 - 0.5) + 0.5x_1x_2 \tag{9}$$

with $x_1, x_2 \in [0,1]$.

A simple constraint, assumed to be directly accessible and not required to be modelled by a surrogate, is imposed as:

$$g(x) = 1 - \frac{x_1 x_2}{0.2} \leq 0 \tag{10}$$

Several runs are performed to assess the influence of number of initial points and level of employed fidelity on the model accuracy and optimization convergence. With 3, 4, 5, 6, and 10 initial points in the high-fidelity model and 20 points in the low fidelity model the convergence progress is shown in Figure 3. The number of iterations is limited to 5, emphasizing the initial phase and the expected advantage of utilizing lower-fidelity information in the model building.

For 50 different initial samples the optimization was performed to eliminate randomness. The mean of the 50 best values at each iteration step was calculated and is shown in Figure 5 for the single and multi-fidelity Kringing approaches with different line types. Additionally, the standard deviation at each iteration was also calculated and is depicted in the same figure as shaded grey area with the same line type for more obvious grouping.

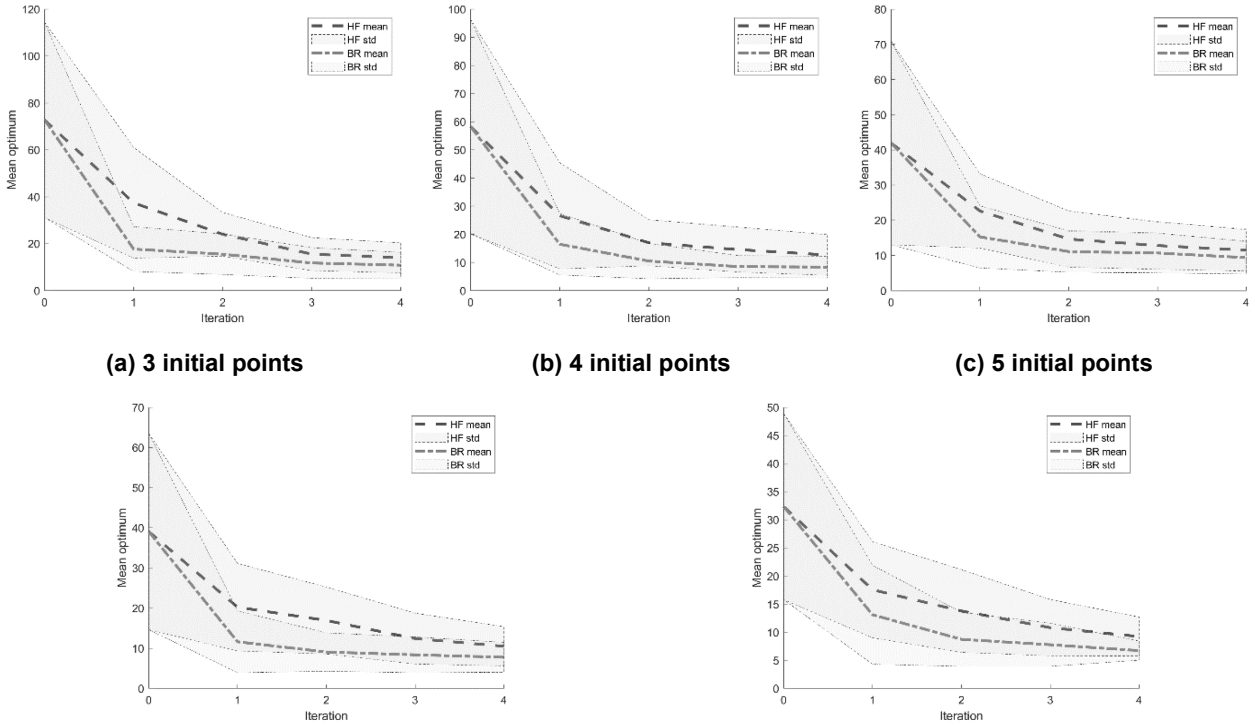

(a) 3 initial points **(b) 4 initial points** **(c) 5 initial points**

(d) 6 initial points **(e) 10 initial points**

Figure 5: Comparison between single (HF) and multi-fidelity (BR) Kringing optimization of the modified Branin function: Mean solution and standard deviation versus iteration.

In all cases it is noticeable that the MF-Kriging model with a bridge function approach (BR) accelerates the convergence and finds improved designs in fewer iterations and with lower uncertainty. It is not clear if a higher initial sample size reduces the uncertainty significantly for both the single- and multi-fidelity approaches. A possible explanation stems from the fact that the uncertainty is highly reduced in the first iterations in the MF approach.

It is therefore apparent that the multi-fidelity approach is beneficial for the identification of regions of minima. Closing in on the global or local optimum is then a matter of tuning the model parameters and possibly reducing the initial design space, and eventually employing different optimization methods as gradient based, for instance.

In the evaluated examples, however, there was no assessment of a global model fitting since for most optimization applications it is seen more suitable to obtain information about regions of minima rather than a fit in the whole design space. Yet is acknowledged that for other applications it can be of interest to have a model representing an expensive function more accurate for the complete design space. This would require a different acquisition function, aiming for the reduction of global error instead of searching for designs of improvement.

Regarding the results using the DNN-MFBO for this test case without including the constraint in (10) and assuming a LF evaluation cost of 10 and HF evaluation cost of 100, it was not possible to obtain any meaningful results with our tentative implementation, neither reproduce the results for the Branin function test case in (Li, 2020).

Not excluding the possibility that the implementation is flawed, there was a severe lack of consistency in the NN results when trained with different initial samples as well as before and after an acquired sample point was added to the training set. It was also not possible to guarantee a consistent set of sample maxima to be used in the computation of the acquisition function.

Consequently, there was no visible trend for convergence or approximation to the maxima, neither to a NN model globally more accurate in representing the high fidelity function. Figure 6 depicts the model results versus the high fidelity function for 5 iterations with an initial set of 20 LF and 5 HF random samples.

Thus, it seems reasonable to admit that a carefully tuned set of training hyper parameters needs to be selected for a successful implementation of the DNN-MFBO methodology and it possibly needs to be changed as the iterations proceed to avoid the dramatic changes in the model outputs. Further investigation is required.

As the DNN-MFBO methodology was unsuccessfully implemented at this point, no further experiments were done with this methodology with the simplified engineering problems reported next.

4.2 Application to the Aeroacoustic Problem

For the scenario of, for instance, an urban air mobility vehicle, the noise generation should be minimized to comply with regulations and reduce environmental impact. Thus, a minimization of the sound pressure level (SPL) is desirable. However, the SPL decreases with disc loading as does the hover power, the outcome of the optimization of the rotor geometrical parameters for SPL minimization tends to be a design limited only by the maximum allowed rotor diameter. Therefore, rotor mass minimization is added to the optimization objective in order to introduce a minimum within the design space. The optimization statement can therefore be stated as following:

$$\begin{aligned} &\text{minimize} && SPL(x) + m_{rotor}(x) \\ &\text{w.r.t.} && x \end{aligned} \tag{11}$$

The design variables vector x contains the rotor solidity and its maximum thickness, the tip Mach number and the disc loading. The high-fidelity assessment considers rotational and vortex noise, while the low-fidelity model only accounts for rotational noise. The computational costs for the aeroacoustic evaluations were low enough to allow for multiple runs with a varying number of initial samples. Similarly to the test functions the convergence towards an optimal point is investigated. The initial samples for the different runs were created as random Latin Hypercube samples, providing a space filling data set of initial evaluations.

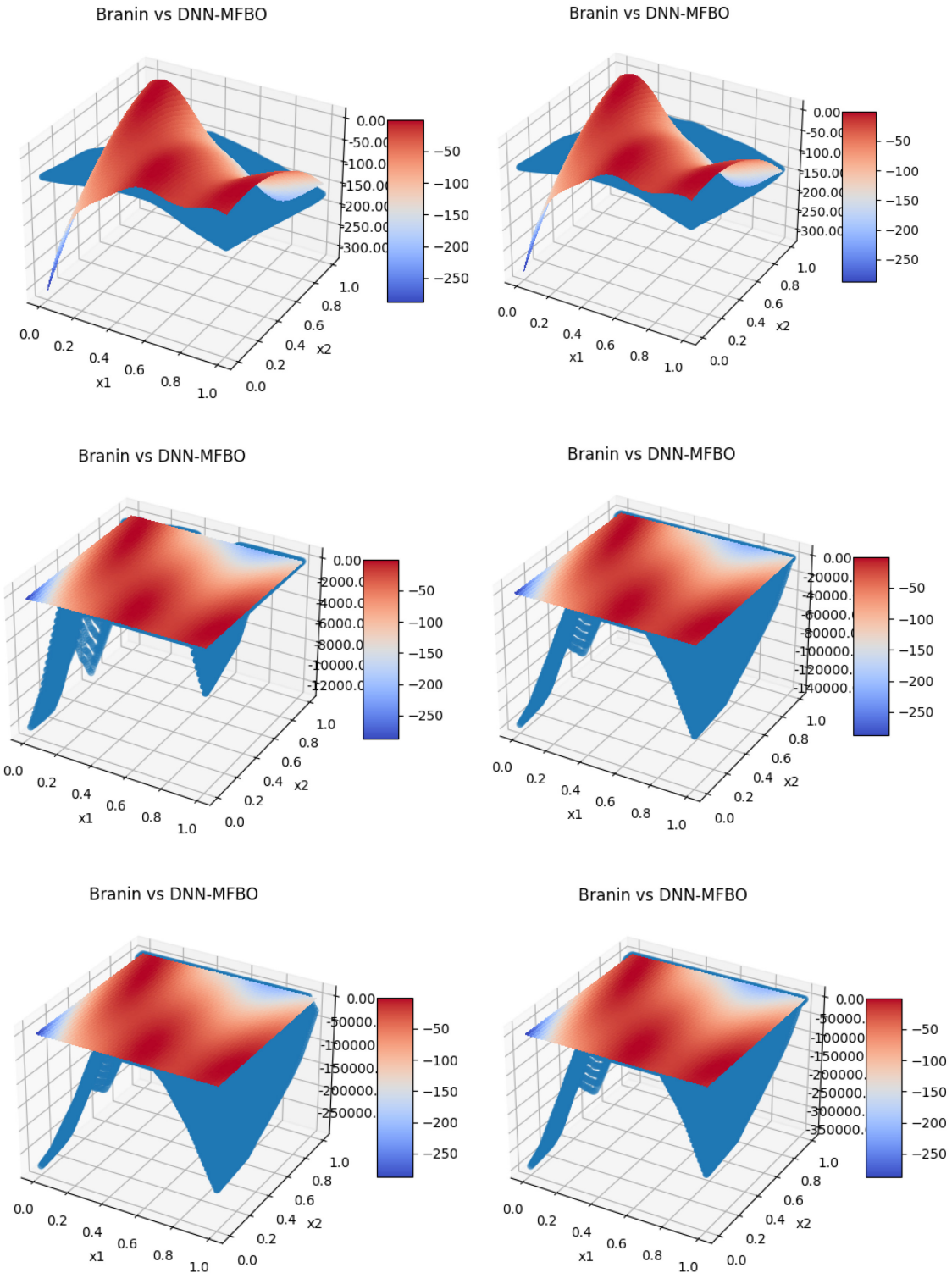

Figure 6: DNN changes after training as more samples are included as the iterations proceed. The iteration number increases from left to right and top to bottom.

Figure 7 shows the convergence for the aeroacoustic problem. For both cases, with 5 and 10 initial samples respectively, the multi-fidelity model approaches an optimum faster than the single-fidelity approach. The standard deviation for the runs is narrower for the multi-fidelity framework, showing that the optimization develops towards an optimum less dependent on the initial samples. This can be attributed to the better fit of the surrogate model and the real function in the early stage of the optimization, allowing a faster closing in on improved design locations.

The results presented below reflect a preliminary optimization considering a single objective SPL minimization with a maximum power constraint and will be updated with the results for the optimization stated above in the final paper version.

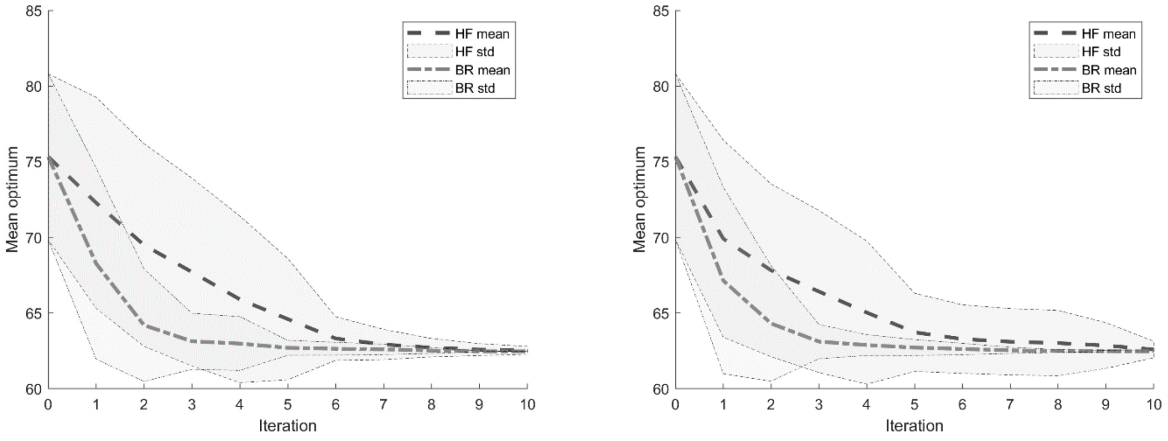

(a) 5 initial points

(b) 5 initial points

Figure 7: Convergence plot for the aeroelastic optimization runs. The convergence of the multi-fidelity bridge method (BR) is faster and with a lower standard deviation than the single-fidelity (HF) convergence.

Figure 8 shows the contour plots of the objective function for the four variable design space of the aeroacoustic problem. The wide black line represents the power requirement constraint. The optimum can be found in the region of high rotor solidity (x_1), low Mach number (x_3) and low disc loading (x_4). The thickness of the rotor (x_2) has a low influence on the noise in the optimum region.

4.3 Application to an Aeroelastic Problem

For the aeroelastic optimization, the objective is a structural mass reduction of a predefined wing outer mold line, constrained by its dynamic response due to a gust load. A stress constraint is included to ensure structural integrity and a binary stability constraint is included prevent a design prone to aeroelastic instabilities. The wing dimensions are given in Table 1.

Table 1: Dimensions of the wing for the aeroelastic optimization problem.

Dimension	Value
Wing span	3m
Mean chord	0.9m
Chord thickness	12%

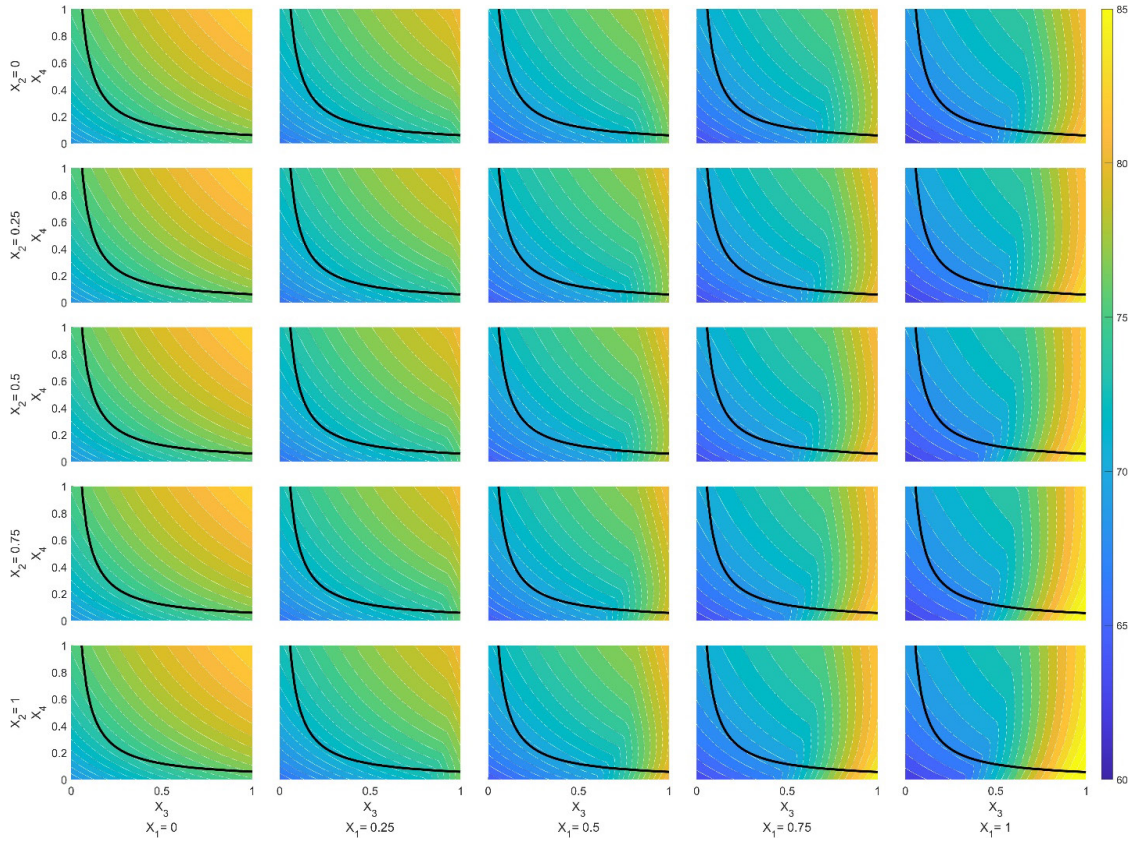

Figure 8: Tiled representation of the 4D aeroacoustic design space.

The steady flight condition is given with an air speed of 20m/s, disturbed by a gust of 2m/s in vertical direction, altering the angle of attack and air speed. The gust is of triangular shape, with a length of 0.5s and the response is monitored up to 0.75s after the gust. The time step for the transient solution is initialized with 0.005s, and is halved if the iterative solver is not able to converge within a time step.

The equivalent beam model of the wing is assumed as box like structure, where the design variables are determining the layout. At three positions along the wingspan the position of the forward and aft spar, the thicknesses of the spars and the thickness of the lower and upper wing skin are utilized as design variables and determine a bilinear distribution of the parameters along the wing span.

$$\begin{aligned} &\text{minimize} && m(x) \\ &\text{w.r.t.} && x \\ &\text{Subject to:} && \frac{\sigma(x,t)}{\sigma_{max}} - 1 \leq 0 \\ & && s(x) - 1 < 0 \end{aligned} \tag{12}$$

With:

$$\begin{aligned} &s(x) = 0, && \text{if stable} \\ &s(x) = 1, && \text{if unstable} \end{aligned} \tag{13}$$

Figure 9 shows the planform of the wing, where the arrows mark the position of the sections where the design variables are defined.

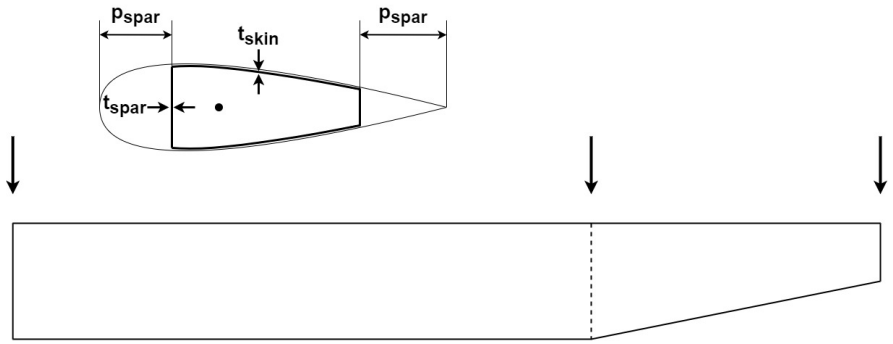

Figure 9: The wing planform for the aerostructural optimization problem. The arrows mark the position on the wing where the design variables of the respective section are defined. Each section has four variables, thus totalizing 12 design variables.

For the optimization a data base of 120 low-fidelity samples was generated. At this point, there were no high-fidelity samples generated. The difference between the low- and high-fidelity assessments is the mesh size for both the aerodynamic and structural models.

The sampling was performed via a Latin-Hypercube for the same space-filling reasons as in the aeroacoustic problem. The assessed high-fidelity samples would be based on the best low-fidelity results to obtain the difference in accuracy between the low- and high-fidelity assessments. Further, as the assessment are based on the same physics-based models, the results would have presumably a similar behaviour and thus the low-fidelity model can be utilized to identify the regions of interest.

For stable design, the gust leads to a deformation as initial response. This can be noticed as the triangular shape of the vertical displacement, the twist and the stress due to the change in load. Afterwards, in a sufficiently damped system, the response dampens back to the static condition, with some minor low amplitude oscillations.

However, if the system's damping is not sufficient it becomes unstable after the initial disturbance, leading to an undamped or negatively dampened response, ultimately causing a failure of the structure.

As mentioned earlier, at this point only the assessment of the accuracy of the low-fidelity Kriging surrogate model has been assessed.

Figure 10 shows an exemplary snapshot of the low fidelity surrogate model for predicting the structural mass and the maximum stress throughout the dynamic gust load response. It is visible that the mass prediction matches the real value well, while the predictions are within the uncertainty bound of one σ. For the stress predictions the values differ more significantly between the predictions and the actual values, showing the challenge of estimating feasible values even with a more elaborate data base of samples.

One more investigation was undertaken considering the eigenfrequencies of the structure. In Figure 11 one can see the prediction for the first 12 eigenfrequencies for the tested wing configurations. While it is a solely structural problem and therefore model, it shows again the complexity of accurately predicting the values. While the magnitude of estimation and actual value are close, differences are partially beyond the uncertainty estimation of one σ. Utilizing those surrogates as low fidelity with the goal to support high--fidelity estimations can jeopardize the whole purpose. Thus, it should be acknowledged that the use of single or multi-fidelity models require a careful assessment of their respective feasibility.

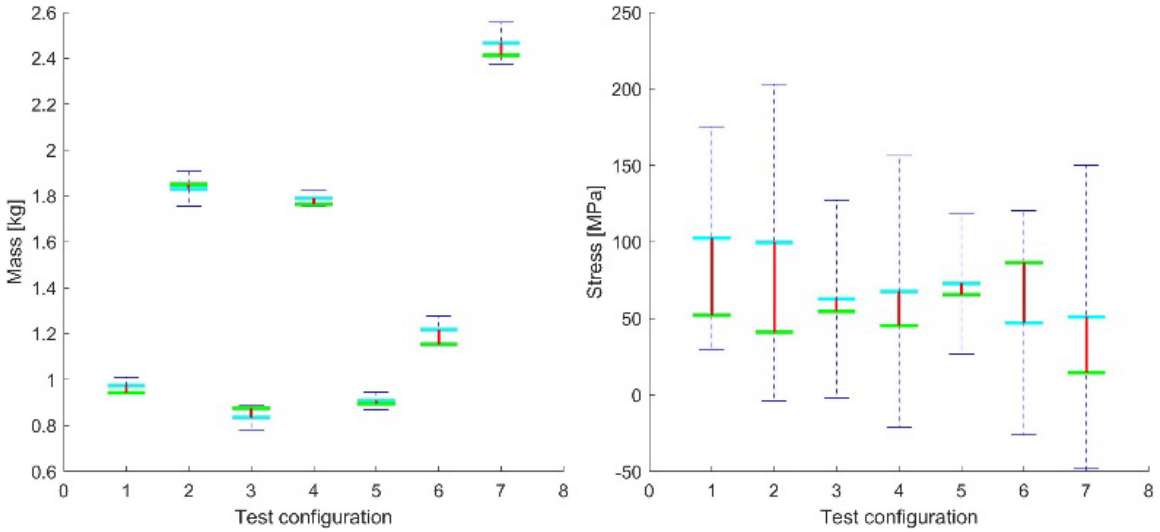

Figure 10: Prediction of structural mass and maximum appearing stress during a dynamic gust load.

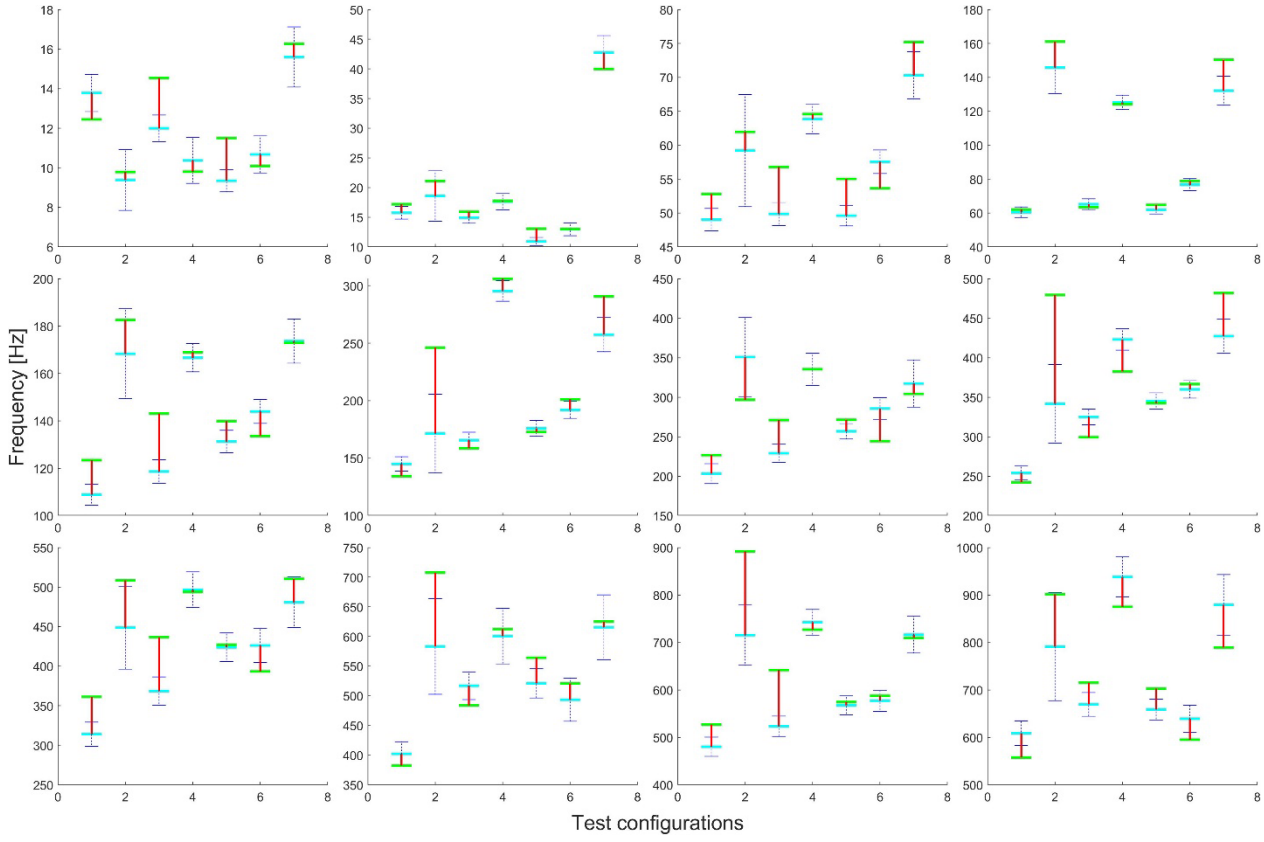

Figure 11: Eigenfrequency prediction for chosen test configurations.

5.0 CONCLUDING REMARKS

So far results indicate that a MF Kriging approach is advantageous when compared to a single fidelity Kriging optimization with the drawback of higher implementation complexity and increased number of tuning parameters.

Similarly to the test functions optimization problems, the more realistic aeroacoustic optimization problem appears to benefit from the multifidelity approach as it approaches the optimum in a lower number of iterations and with lower uncertainty.

A definite conclusion on the computational costs of the single- vs multi-fidelity Kriging approaches cannot be drawn because there is a balance between the low and high-fidelity evaluations that might tend towards one approach or the other, mostly influenced by the cost ratio between low and high-fidelity evaluation.

Regarding the DNN-MFBO framework, it was unsuccessfully implemented as a result of what we believe to be high sensitivity to the NN architecture and tuning parameters in the training phase of the optimization iterations and to the sampling.

Open questions regarding the employment of multi-fidelity approaches still remain. Those include the balance between the low and high-fidelity evaluations, mostly influenced by the cost ratio between them.

However, many aspects of a decision for one approach over the other have to be made *a priori* to an optimization when details about the performance are not yet known.

A robust method is therefore more often preferred as the implementation can be time-intensive, and changes later on due to robustness issues can eliminate contemplated benefits.

6.0 FUTURE WORK

Research activities will continue with the application of MF Kriging to the aerostructural optimization problem and of the DNN-MFBO approach to the test functions and engineering optimization cases.

Effects of the level of correlation between high and low fidelity models need to be investigated, specifically for the MF-Kriging approach where simpler correlation

Further DNN-MFBO framework improvement attempts need to be made, namely in the architecture and hyper parameters optimization prior to training and MF optimization.

7.0 REFERENCES

Berke, Patnaik and Murthy (1993).”Application of Artificial Neural Networks to the Design Optimization of Aerospace Structural Components.” NASA Technical Memorandum 4389.

Bouhlel, M.A., Bartoli, N., Otsmane, A., & Morlier, J. (2016). “Improving kriging surrogates of high-dimensional design models by Partial Least Squares dimension reduction.” Structural and Multidisciplinary Optimization, *53*(5), Pages 935-952.

Brown, A., Harris, W. (2018), A Vehicle Design and Optimization Model for On-Demand Aviation, in: AIAA/ASCE/AHS/ASC Structures, Structural Dynamics, and Materials Conference, Kissimmee, FL, USA. doi:10.2514/6.2018-0105

Dong, Y (2018). "An application of Deep Neural Networks to the in-flight parameter identification for detection and characterization of aircraft icing." Aerospace Science and Technology, Volume 77, June 2018, Pages 34-49. https://doi.org/10.1016/j.ast.2018.02.026

Giselle Fernández-Godino, M., Park, C., Kim, N. H., and Haftka, R. T. (2019). "Issues in deciding whether to use multifidelity surrogates." *AIAA Journal*, *57*(5), 2039-2054.

Kandasamy K., Dasarathy G. Oliva J. B. et al. (2016), "Gaussian process bandit optimization with multi-fidelity evaluations". Advances in Neural Information Processing Systems, pp. 992-100.

Kandasamy K., Dasarathy G. Shneider J. et al. (2017) "Multi-fidelity Bayesian optimization with continuous approximations". Proceedings of the 34th International Conference on Machine Learning-Volume 70 pp. 1799-1808.

Song, J., Chen, Y., and Yue, Y. (2019, April). "A general framework for multi-fidelity bayesian optimization with gaussian processes". In *The 22nd International Conference on Artificial Intelligence and Statistics* (pp. 3158-3167). PMLR.

Li, S., Xing, W., Kirby, R., and Zhe, S. (2020). "Multi-fidelity Bayesian optimization via deep neural networks." *Advances in Neural Information Processing Systems*, *33*, 8521-8531.

Takeno, S. et al. (2020) "Multi-fidelity Bayesian Optimization with Max-value Entropy Search and its parallelization" arXiv:1901.08275. https://doi.org/10.48550/arXiv.1901.08275

Meliani, Mostafa, et al. (2019) "Multi-fidelity efficient global optimization: Methodology and application to airfoil shape design." AIAA aviation 2019 forum.

Rumpfkeil, Markus P., and Philip S. Beran (2020). "Multi-fidelity, gradient-enhanced, and locally optimized sparse polynomial chaos and kriging surrogate models applied to benchmark problems." AIAA Scitech 2020 Forum. doi:10.2514/6.2020-0677

Secco and Mattos (2015). "Artificial Neural Networks Applied to Airplane Design." 53rd AIAA Aerospace Sciences Meeting, 5-9 January, 2015, Florida USA. https://doi.org/10.2514/6.2015-1013

Renganathan, S. Ashwin, Maulik, Romit, and Ahuja, Jai (2021). "Enhanced data efficiency using deep neural networks and Gaussian processes for aerodynamic design optimization". United States: N. p., 2021. doi:10.1016/j.ast.2021.106522

Sobester, András, Alexander Forrester, and Andy Keane (2008). Engineering design via surrogate modelling: a practical guide. John Wiley & Sons.

Zhang, Xinshuai, et al. (2021) "Multi-fidelity deep neural network surrogate model for aerodynamic shape optimization." Computer Methods in Applied Mechanics and Engineering 373: doi:10.1016/j.cma.2020. 113485